655. A non-parametric hysteresis model for magnetorheological dampers

Ardeshir Karami Mohammadi, Mohammad Sheibani
Department of Mechanical Engineering, Islamic Azad University of Iran, Karaj Branch, Karaj, Iran
E-mail: *akaramim@yahoo.com*

(Received 05 July 2011; accepted 1 September 2011)

Abstract. In this paper a new non-parametric hysteresis model is offered for simulation of behaviors of magneto-rheological dampers. The offered model takes the excitation frequency, amplitude and current as variables and because of that it is capable of estimating the hysteresis force in different stimulation conditions with a good level of accuracy. Also, the model has the required level of flexibility for simulation of different dampers. The model completion is free of all complications observed in other models. Finally, the accuracy of simulations provided by this model are compared with experimental data as well as two parametric and non-parametric models.

Keywords: magnetorheological damper, hysteresis, non-parametric model.

1. Introduction

Magneto-rheological (MR) dampers are semi-active control tools that have received a lot of attention in recent years due to their structural simplicity, wide range of applications, low energy consumption, high capacity and high reliability. Automobile suspension and structural vibration control systems are among the most frequent uses of such dampers. The main challenge to the expansion of using these dampers is presenting a model capable of simulating their non-linear and complex hysteresis behaviors in a suitable manner. So far many different models have been presented for simulation of hysteresis of magneto-rheological dampers. Models such as Bouc-Wen parametric model and other non-parametric models are based on sigmoid functions. Nevertheless, many of these models demonstrate differences between results of experimental tests and simulations. Also, in most models the model characterizing parameters are not functions of frequency, amplitude and current of stimulation. Thus they must be recalculated for different stimulation conditions. Shames and Cozarelli [1] presented a model that used a dry friction element in parallel with a viscous damper, known as the Bingham Visco-Plastic model. Gamato and Filisko [2] presented their parametric viscoelastic-plastic model based on Bingham's model. Ehrgott and Masri [3] and Gavin *et al* [4] used Chebychev's polynomials to present a non-parametric method for estimation of controllable fluid damper through the use of displacement and damper velocity data. Wereley *et al* [5] presented a linear hysteresis bi-viscous model with improvements in its pre-yield hysteresis accuracy in comparison to bi-viscous models. Choi and Lee [6] developed a polynomial model in which only the stimulation current was taken as the model variable. Despite its structural simplicity that made simplified the task of control system designer, this model suffers from low simulation accuracy [10]. The Bouc-Wen model [8] has been frequently used to simulate the behaviors of magneto-rheological dampers. Yet one of the main problems with this model is the calculation of its unknown parameters. A range of methods have been proposed to determine these parameters such as the trial and error or some optimization techniques such as SQP, all aimed at minimizing the discrepancies between experimental and simulation results. In this method the combination of parameters to be optimized creates a large solution space for which there is normally no accurate and agreed solution. In other words, because the search space covers a large range, the final answer cannot necessarily be fitted with the hysteresis phenomenon. Therefore, sometimes there are considerable differences between experimental and simulation

results [6, 9]. Moreover, characteristic parameters of Bouc-Wen model are not functions of excitation current, amplitude and frequency, and estimated parameters can only simulate the damper behaviors in special circumstances. Spenser *et al* [9] offered his optimized model based on the Bouc-Wen model. It identifies damper behaviors at lower velocities with better accuracy than the Bouc-Wen model, and it is a function of the stimulation current too. Like Bouc-Wen, Spenser's model is known as a model associated with permanent problems in finding the required parameters [7]. The goal of this paper is the offer an accurate model for simulation of magneto-rheological dampers behaviors that takes into account the excitation current, amplitude and frequency as input variables. The newly offered model is capable of estimating the damper force for any combination of excitation current, amplitude and frequency. Given the special characteristics of this model, identification of its parameters is not such a hard task because their approximate values may be easily calculated according to primary experimental data. Also, the final accuracy of the model is controllable during the modeling process, and the offered model has a high degree of flexibility which makes the modeling process easier.

2. Presented Model

This model is based on simulation of force-velocity hysteresis behavior of magneto-rheological dampers. Many of the models presented so far have taken the same approach to modeling [6, 7, 10]. In the presented model, modeling includes several separated stages in the following order.

2.1. Creating a Base Model

First we need a base model capable of covering with sufficient accuracy the hysteresis phenomenon of the force-velocity curve for different excitation currents, frequencies, and amplitudes through changing the model parameters. For instance, the Bouc-Wen model or other models using sigmoid functions to model damper behaviors may be good choices for a base model.

The base model used here is of linear type. As observed in Fig. 1, the model consists of 6 separate linear functions. Since modeling for negative accelerations is done on the force-velocity curve, according to Fig. 1 four key points *A*, *B*, *C*, and *D* are taken on the force-velocity curve. *A* represents the maximum force at positive velocity, *D* represents maximum force for negative velocity, *B* represents yield force at positive velocity, and *C* represents yield force at negative velocities. Also, *C** and *B** points are the images of *B* and *C* points in relation to the coordinate system reference point. As can been observed in Fig. 1, the base function for modeling consists of six separate linear functions passing through all points highlighted in the model. Thus the base modeling function is expressed in the following way:

for negative accelerations:

$$F_d = \begin{cases} y_A + h_a(\dot{x} - x_A); & \dot{x} > x_B \\ y_B + h_b(\dot{x} - x_B); & x_C < \dot{x} < x_B \\ y_C + h_c(\dot{x} - x_C); & \dot{x} < x_C \end{cases} \quad (1)$$

for positive accelerations:

$$F_d = \begin{cases} y_A + h_{a^*}(\dot{x} - x_A); & \dot{x} > -x_C \\ -y_C + h_b(\dot{x} + x_B); & -x_B < \dot{x} < -x_C \\ y_D + h_{c^*}(\dot{x} - x_D); & \dot{x} < -x_B \end{cases} \quad (2)$$

where F_d is the damper force and also:

$$h_a = (y_A - y_B)/(x_A - x_B) \tag{3}$$

$$h_b = (y_B - y_C)/(x_B - x_C) \tag{4}$$

$$h_c = (y_C - y_D)/(x_C - x_D) \tag{5}$$

$$h_{a^*} = (y_A + y_C)/(x_A + x_C) \tag{6}$$

$$h_{c^*} = (y_D + y_B)/(x_D + x_B) \tag{7}$$

In the above equations the longitudinal coordinates of A, D (x_A, x_D) are calculated as follows:

$$x_A = -x_D = \dot{x}_m \tag{8}$$

where x, $\dot{x}$, and $\ddot{x}$ are position, velocity and acceleration of the damper. $\dot{x}_m$ is the maximum damper velocity calculated from the following equation:

$$\dot{x}_m = 2\pi.a.f = \sqrt{\dot{x}^2 - x.\ddot{x}} \tag{9}$$

where a is the amplitude and f is the frequency of stimulation.

Therefore by having the longitudinal positions of B and C (i.e. parameters x_B and x_C) and latitudinal positions of A, B, C, and D (i.e. y_A, y_B, y_C, and y_D) we can simulate the model completely. The model has six unknown parameters which change according to current, amplitude and frequency of stimulation.

To fit the base model over experimental samples, we need to find the six parameters x_C, x_B, y_D, y_C, y_B and y_A.

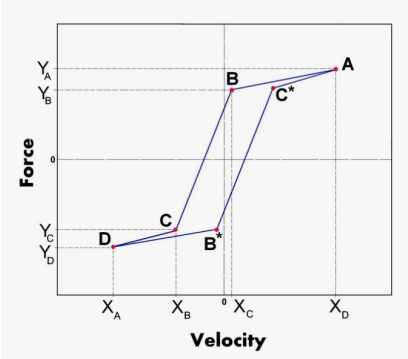

Fig. 1. Base model function

Given the simplicity of the base function the approximate values of each model parameter can easily be estimated from experimental data for different stimulation conditions. So fitting the model for different stimulation conditions on experimental curves, either by trial and error or by practical optimization techniques, will not be such a hard task after all. This is another advantage of the presented model over other models such as Spenser's.

2.2. Calculation of Model Parameters

To calculate model parameters we need experimental data obtained for different currents, frequencies and ranges of stimulation. To complete the model we first need to take one current, one amplitude and one frequency as the zero excitation condition. Zero excitation condition may be taken as an average range of any excitation conditions. For example, if the excitation current ranges from 0 to 1.5 A, 0.75 A is taken as the zero excitation current. Also, zero

excitation values for each condition may be considered to be equal to the value for which maximum excitation occurs. For instance, if excitation frequency ranges from 0.5 to 1.5 Hz but maximum applied frequency is between 0.5 and 7.5 Hz, then 5 Hz will be a good choice for zero excitation frequency. Once the zero excitation conditions are set it is time to obtain the required experimental data for the model. To do this we must suppose that one of the triple excitation conditions is variable and the other two are zero and then test the damper to obtain the needed data. This is repeated for all excitation conditions. Thus the data required for modeling are three group of force-velocity curves each having one different stimulation condition as variable and the other two as zeroes.

One model that uses amplitude and frequency besides the current in its modeling is represented by Wang *et al* [7]. X. Q. Ma et al optimized Wang's model and compared his model accuracy with those of corrected Bouc-Wen. In this paper the modeling is performed over experimental data provided by X. Q. Ma *et al* (Fig. 2) so that the accuracy of the presented model may be compared not only to experimental data but also by X. Q. Ma and Bouc-Wen's corrected models.

Now it is time to fit the base model over experimental curves to obtain the model parameters. Because experimental data are functions of stimulation current, frequency and amplitude, once the model is fitted on all experimental data, each model parameter will be a function of three variables: stimulation current, frequency and amplitude, unless it is made clear after the fitting process that one or more of model parameters are not functions of some stimulation conditions. In this paper the fitting of model over experimental data is done by trial and error method.

2.3. Calculation of Parameter Change Function

In this section for each model parameters and each stimulation condition a function is passed over the points obtained after fitting the base model over experimental data. For instance, for parameter y_A which is a function of all three stimulation conditions, we pass it through all experimental points in all different conditions of variable current, variable amplitude and variable frequency.

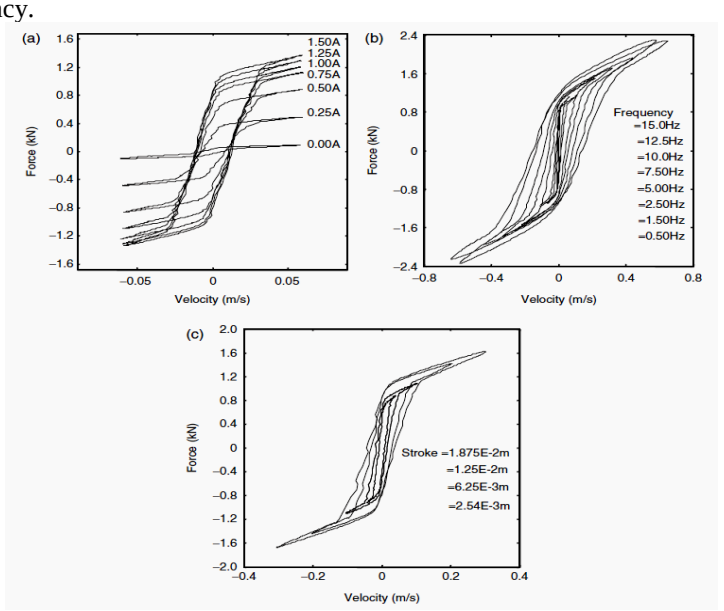

Fig. 2. Force-velocity curves measured for MR damper at stimulation conditions (a) 6.35 mm and 1.5 Hz, (b) 6.35 mm and 0.75 *A*, (c) 2.5 Hz and 0.75 *A*. (from X. Q. Ma *et al*, 2007)

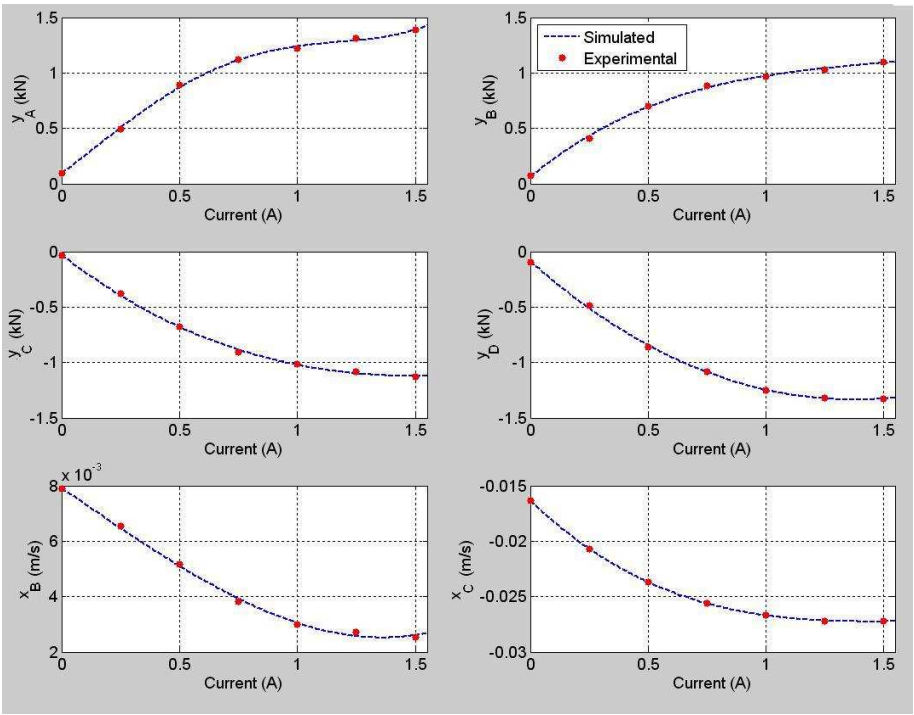

Fig. 3. Polynomial functions fitted over experimental data of model parameters for variable current and a=6.35 mm, f=1.5 Hz

Passed functions are functions of the polynomial and their maximum exponent is four. Functions passed through points related to variable frequency are slightly different due to the complexity of the passing function.

Figure 3 shows the functions fitted over experimental values of model parameters in different currents. The overall form of the functions is as follows:

$$Z_i(i) = c_{11}i^4 + c_{12}i^3 + c_{13}i^2 + c_{14}i + c_{15} \quad (10)$$

where Z_i is model parameter, i is stimulation current, and c_{11}, c_{12}, c_{13}, c_{14}, c_{15} are constant coefficient for each mode parameter taken from Table 1.

Figure 4 presents the functions fitted over experimental values of model parameters in different amplitudes. The overall form of the functions is as follows:

$$Z_a(a) = c_{21}a^3 + c_{22}a^2 + c_{23}a + c_{24} \quad (11)$$

where Z_a is model parameter, a is stimulation amplitude, and c_{21}, c_{22}, c_{23}, c_{24} are constant coefficient for each mode parameter taken from Table 2.

Figure 5 shows the functions fitted over experimental values of model parameters in different frequencies. Since changes in model parameters for frequency are more complex that the previous two cases, the fitted functions are a little more complex. Thus the overall form of the functions consists of two sections, the first being a polynomial of the following format:

$$Z_f^*(f) = c_{31}f^3 + c_{32}f^2 + c_{33}f + c_{34} \quad (12)$$

The second section of the function is an exponential function multiplied in the first function. The overall form of the functions is as follows:

$$Z_f(f) = Z_f^*(f) \times \left(d_1.\exp(d_2.(f + d_3)^2) + 1\right) \quad (13)$$

where Z is model parameter, f is stimulation frequency, and c_{31}, c_{32}, c_{33}, c_{34}, d_1, d_2, d_3, are constant coefficient for each mode parameter taken from Table 3.

Table 1. Polynomial constant coefficients for variable current

	Z					
	y_A	y_B	y_C	y_D	x_B	x_C
c_{11}	0.6526	0	0	0	0	0
c_{12}	-1.705	0.2533	-0.08733	-0.03493	0.001146	-0.002419
c_{13}	0.6023	-1.08	0.7448	0.7535	-2.025e-4	0.01223
c_{14}	1.596	1.736	-1.625	-1.879	-5.822e-3	-0.02017
c_{15}	0.09428	0.06339	-0.02713	-0.08569	7.927e-3	-0.01634

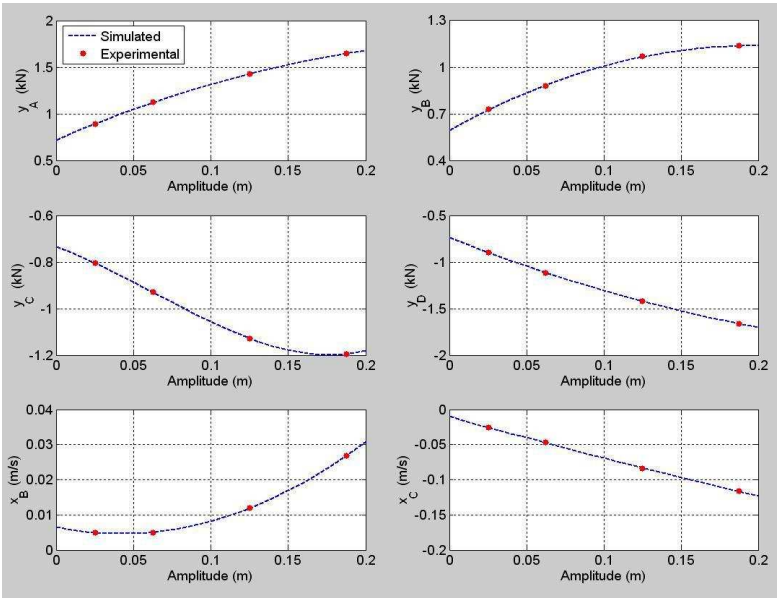

Fig. 4. Polynomial functions fitted over experimental data of model parameters for variable amplitude and i=0.75 A, f=1.5 Hz

Table 2. Polynomial constant coefficients for variable amplitude

	Z					
	y_A	y_B	y_C	y_D	x_B	x_C
c_{21}	0	0	89.79	0	0	0
c_{22}	-11.62	-13.99	-17	8.541	1.051	0.2497
c_{23}	7.128	5.527	-2.431	-6.523	-0.08838	-0.615
c_{24}	0.7196	0.594	-0.7336	-0.7386	6.501e-3	-0.01005

Accuracy of functions fitted over obtained values plays the major role in our model accuracy. The important point is that the fitted function must be approximated at a high level of accuracy with related points under zero stimulation conditions, even if we need to approximate the other points with lower levels of accuracy, because the points have key influence on the model.

2.4. Calculation of Multivariable Functions for Parameters

So far the relation between each model parameter and related excitation conditions affecting that parameter was obtained separately. Now it is time to convert these separate relations into one multivariable function from excitation conditions of each single model parameter. For

instance, y_A parameter is a function of any excitation condition that may be expressed in the following manner:

$$y_A(a, i_0, f_{02}) = F(a) \tag{14}$$

$$y_A(a_0, i, f_{01}) = G(i) \tag{15}$$

$$y_A(a_0, i_0, f) = K(f) \tag{16}$$

where a is amplitude variable, i is current and f is frequency variable, and i_0, a_0, f_{01}, and f_{02} are zero values of excitation conditions. It must be pointed out here that we can take two zero excitation values only for one excitation condition. For instance, here the two zero excitation values of f_{01} and f_{02} are taken for frequency. This increases the accuracy of damper behavior recognition for this special excitation condition. The same can be done for excitation condition which includes a large range of changes or whose change introduces special complications into damper behaviors.

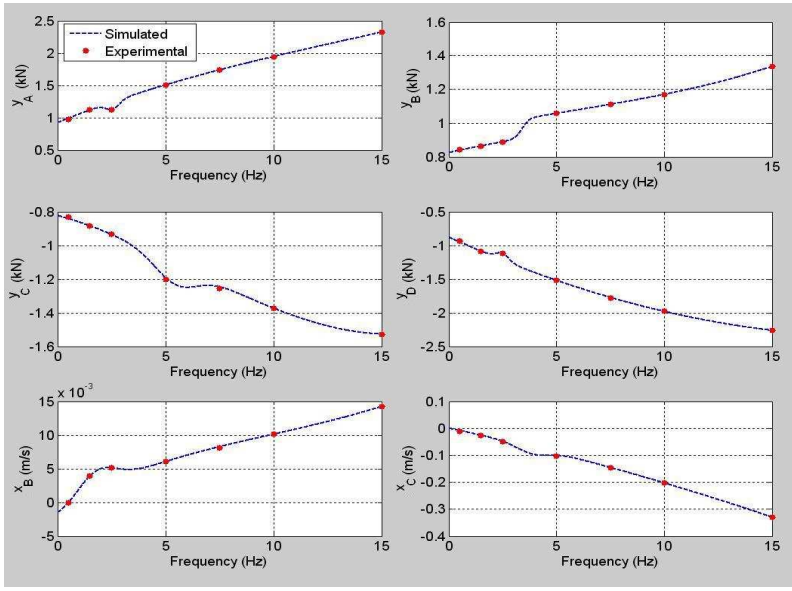

Fig. 5. Functions fitted over experimental data of model parameters for variable frequency and i=0.75 A, a=6.35 mm

Table 3. Polynomial and exponential constant coefficients for variable frequency

	Z					
	y_A	y_B	y_C	y_D	x_B	x_C
c_{31}	1.1101e-4	1.309e-4	2.395e-4	0	0	0
c_{32}	-4.522e-3	0.003264	-4.377e-3	3.625e-3	-1.1159e-4	3.39e-4
c_{33}	0.1364	0.01385	-0.03523	-0.1469	1.87e-3	-0.01691
c_{34}	0.9223	0.8363	-0.8218	-0.8741	-8.98e-4	3.56e-4
d_1	-0.091	0.0975	0.115	-0.0825	1.419	0.37
d_2	-5.292	-0.292	-0.532	-5.292	-0.5	-0.92
d_3	-2.54	-5.73	-5.43	-2.49	-1.246	-3.746

Given (14), (15) and (16) we have:

$$G(i_0) = K(f_{01}) \tag{17}$$

$$F(a_0) = K(f_{02}) \tag{18}$$

So y_A may be expressed as the following three-variable function:

$$y_A(a, i, f) = \frac{F(a).G(i).K(f)}{F(a_0).G(i_0)} \tag{19}$$

It can easily be shown that equation (19) covers all three equations of (14), (15) and (16).

According to Figure 2 on which modeling is done, the zero stimulation parameters are chosen as follows:

$$i_0 = 0.75A, a_0 = 6.35mm, f_{01} = 1.5Hz, f_{02} = 2.5Hz \tag{20}$$

Now according to equation (18) we can express each model parameter in the form of a multivariable function of excitation conditions. Replacing the obtained equations in the base model (equations (1) to (7)) with then give us a complete model whose parameters are all functions of excitation conditions.

3. Model Evaluation

In this part we do a comparison between simulation of the presented model and experimental data, and another comparison between the presented model and two models of X.Q. Ma *et al* and Bouc-Wen [10].

Figure 6 provides the comparison of results obtained from damper behavior simulation and experimental data for variable current, frequency and amplitude. As can be observed there is a good correlation between model and experimental data. Experimental data used in this figure are the same on which the modeling was based.

To ensure that the presented model is capable of simulating damper behaviors under any excitation conditions, figure 7 provides a comparison between experimental data and results of model simulation in different excitation conditions. Here too our model offers a very nice simulation.

To compare the accuracy of presented model with X. Q. Ma *et al* and Bouc-Wen models [8, 9], the behavior simulated by the two models and experimental data for variable frequency and constant current were compared in Figure 8 (data required for Bouc-Wen were taken from [7]). It is observed that the two models lack a good level of accuracy for excitation conditions different with that they were based on.

4. Conclusions

In this paper a new hysteresis model was reported for simulation of magneto-rheological dampers under different excitation conditions. The proposed model contains several exclusive innovations. Since modeling is done through choosing 4 key points (A, B, C, D) over the force-velocity curve of the damper, model parameters are easily extractable. Thus there is no need to use optimization procedures. Moreover, each model parameter changes incrementally or decrementally according to excitation conditions, which facilitates the modeling process.

Also, here a linear function was used as a base function, but the presented method is not bound to use such a function and may well use any other function suitably fitted to force-velocity curves of the damper, and that is because the next steps of modeling are independent of the type of base function.

Accuracy of the function fitted over experimental data for each model parameter determines the final accuracy of the model, so increase of accuracy will result in increased complexity of

the functions related to model parameters. Also, the presented model has several stages of completion with high flexibility.

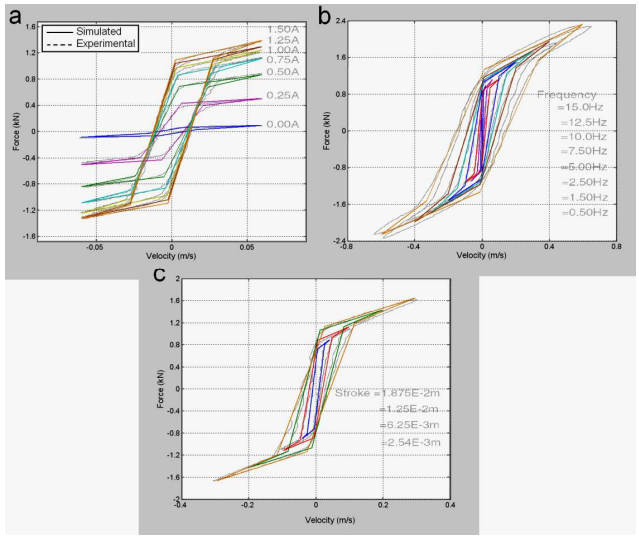

Fig. 6. Comparison between simulation results and experimental data for (a) 1.5 Hz and 6.35 mm (b) 6.35mm and 0.75 A (c) 2.5 Hz and 0.75 A (experimental data from X. Q. Ma *et al*, 2007)

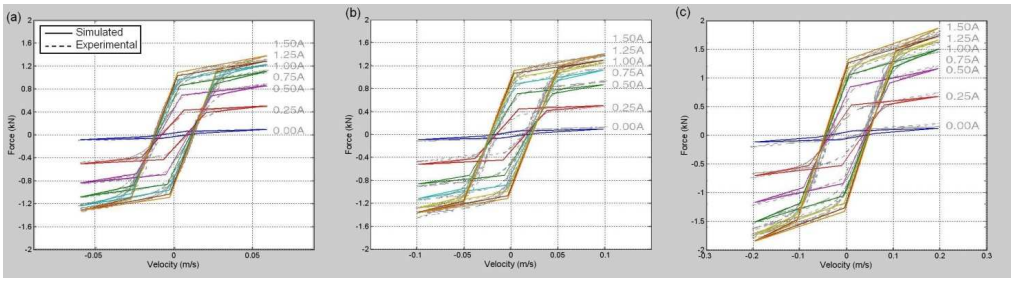

Fig. 7. Comparison between simulation results and experimental data for 6.35 mm and (a) 1.5 Hz, (b) 2.5Hz, (c) 5Hz (experimental data from X. Q. Ma *et al*, 2007)

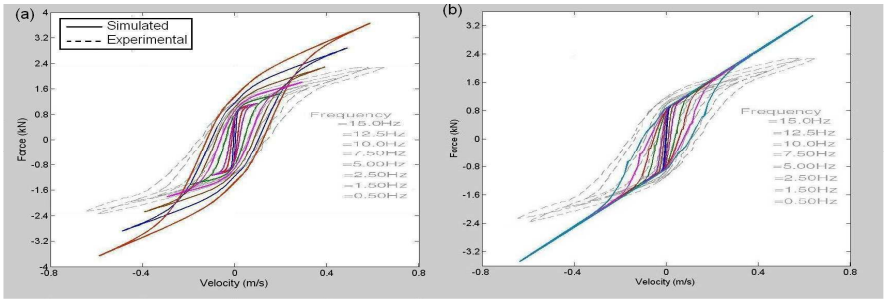

Fig. 8. Comparison between simulation results and experimental data in stimulation conditions 2.5 Hz and 0.75A for (a) by model Xia, 2007, (b) corrected Bouc-Wen model (experimental data from X. Q. Ma *et al*, 2007)

The model may be used for any type of magneto-rheological damper with any given accuracy. Other characteristics of the model include simplicity in the modeling process and

guaranteed final accuracy in comparison to other models that need optimization of model parameters in an infinity space, making them both time consuming and poorly accurate.

References

[1] Shames I. H. and Cozzarelli F. A.1997 Elastic and Inelastic Stress Analysis, Taylor & Francis, N. J.

[2] Gamato D. R. and Filisko F. E. 1991 Dynamic mechanical studies of electrorheological materials: moderate frequencies, J. Rheol., 35, p. 399–425.

[3] Ehrgott R. and Masri S. F. 1992 Modeling the oscillatory dynamic behaviour of electrorheological materials in shear, Smart Mater. Struct., 1, p. 275–85.

[4] Gavin H. P., Hanson R. D. and Filisko F. E. 1996 Electrorheological dampers, Part 1: analysis and design, J. Appl. Mech. ASME, 63, p. 669–75.

[5] Wereley N. M. and Pang L. 1998 Nondimensional analysis of semi-active electrorheological and magnetorheological dampers using approximate parallel plate models, Smart Mater. Struct., 7, p. 732–43.

[6] Choi S. B. and Lee S. K. 2001 A hysteresis model for the field-dependent damping force of a magnetorheological damper, J. Sound Vib., p. 375–83.

[7] Wang E. R., Ma X. Q., Rakheja S. and Su C. Y. 2003 Modeling the hysteric characteristics of a magnetorheological fluid damper, Proc. IMechE D: J. Automobile Eng., 217, p. 537–50.

[8] Wen Y. K. 1976 Method of random vibration of hysteretic systems, J. Eng. Mech. ASCE, 102, p. 249–63.

[9] Spencer B. F. Jr., Dyke S. J., Sain M. K. and Carlson J. D. 1997 Phenomenological model for a magnetorheological damper, J. Eng. Mech. Am. Soc. Civil Eng., p. 230–52.

[10] Xiao Qing Ma, S. Rakheja and Chun-Yi Su 2007 Development and Relative Assessments of Models for Characterizing the Current Dependent Hysteresis Properties of Magnetorheological Fluid Dampers, J. of Intelligent Material Systems and Structures, 18, p. 487–50.

[11] Shuqi Guo, Shaopu Yang and Cunzhi Pan 2006 Dynamic Modeling of Magnetorheological Damper Behaviors, Journal of Intelligent Material Systems and Structures, 17; 3.

[12] Dominguez A., Sedaghati R. and Stiharu I. 2004 Modeling the hysteresis phenomenon of magnetorheological dampers, Smart Mater. Struct., 13, 1351.

[13] Xubin Song, Mehdi Ahmadian and Steve C. Southward 2005 Modeling Magnetorheological Dampers with Application of Nonparametric Approach, Journal of Intelligent Material Systems and Structures, 5, p. 421-432.

[14] Sims N. D., Holmes N. J. and Stanway R. 2003 A unified modeling and model updating procedure for electrorheological and magnetorheological vibration dampers, Journal of Smart Mater. Struct., 13, 100.

[15] Dominguez A., Sedaghati R. and Stiharu I. 2006 A new dynamic hysteresis model for magnetorheological dampers, Journal of Smart Mater. Struct., 15, 1179.

